Finite Fracture Mechanics: a deeper investigation on negative T-stress effects

Finite Fracture Mechanics: A deeper investigation on negative T-stress effects

A. Sapora , V. Mantič

Department of Structural, Geotechnical and Building Engineering, Politecnico di Torino, Corso Duca degli Abruzzi 24, 10129, Torino, Italy

Group of Elasticity and Strength of Materials, School of Engineering, Universidad de Sevilla, Camino de los Descubrimientos s/n, 41092, Sevilla, Spain

Abstract

In the present work, the coupled stress and energy criterion of Finite Fracture Mechanics (FFM) is applied to investigate negative T-stress effects related to mixed-mode brittle fracture of cracked elements. Only two material parameters are involved in the analysis, the tensile strength and the fracture toughness, which are independent of the mode-mixity. Below a critical T-value, the shear contribution to the strain energy release rate (ERR) starts to prevail in the mode II-dominated zone. This affects FFM **results** in terms of: (i) the fracture loci, with the critical mode II-stress intensity factor (SIF) never exceeding the fracture toughness; (ii) the critical kinking angle and the actual crack advance (which results to be a structural parameter), both decreasing to infinitesimal quantities as mode II- loading conditions are approached. **These predictions can be revised by considering a large amount of energy dissipated under mode II loading conditions and by assuming a mode-mixity dependent ERR. A discussion on experimental data for brittle and quasi-brittle materials available in the literature is included.**

Email address: alberto.sapora@polito.it, mantic@us.es (A. Sapora , V. Mantič)

Keywords: Mixed-mode brittle FFM, crack kinking, negative T-stress, ERR

1. Introduction

Effects of T-stress on mixed-mode brittle fracture of cracked elements have been extensively investigated by means of models combining a linear-elastic analysis with an internal material length. The simple point stress criterion was considered in Kosai et al. (1993); Seweryn (1998) and later developed and applied to different experimental data in Smith et al. (2001, 2006), where it was renamed as Maximum Tangential Stress (MTS) criterion. Nonlocal (average) stress and energy approaches were formalized by Seweryn (1998), although the internal critical distance related to the latter was apparently underestimated (Pugno and Ruoff, 2004). Stress and energy criteria, despite their simplicity and general accuracy, remain distinct and the fulfilment of one of them usually implies the violation of the other one: this could lead to some drawbacks, as pointed out in Carpinteri et al. (2008). **For a detailed overview on T-stress effects in fracture mechanics, see Gupta et al. (2015) and therein references.**

More recently, also FFM approaches coupling the energy balance with a stress requirement, either punctual (Leguillon, 2002) or averaged (Cornetti et al., 2006), were proposed in this framework. One of the most important feature related to FFM is that the crack advance becomes a structural parameter, depending also on the geometrical characteristics (Carpinteri et al., 2011; Sapora et al., 2013). In order to take T-stress effects into account, the coupled criterion proposed by Leguillon was developed numerically (Leguillon and Murer, 2008), by a two-scale asymptotic matching procedure (Leguillon, 1993). On the other hand, a semi-analytical approach was adopted by Cornetti et al. (2014), by implementing the

angular functions tabulated in Tada et al. (1985); Melin (1994), the approximating expressions of which can be found in Amestoy and Leblond (1992). Eventually, FFM was applied to investigate T-stress effects on crack bifurcation phenomena in ceramic laminates by Ševeček et al. (2014).

From a qualitative point of view, theoretical models all predict the same general behavior for a positive T-stress: it decreases both the failure load and the critical kinking angle. In case of pure mode I loading conditions, if $T \geq T^* > 0$ the crack ceases to propagate collinearly and the critical value of mode I-SIF K_{If} deviates smoothly from the material fracture toughness K_{Ic} (Smith et al., 2001; Leguillon and Murer, 2008; Cornetti et al., 2014), see also the stability analysis carried out in Cotterell and Rice (1980). Estimations for the threshold T^* differ slightly between each other according to the implemented failure criterion.

An opposite trend is observed for negative T-stresses. Indeed, according to stress-based criteria, the critical value of mode II-SIF K_{IIf} can exceed K_{Ic} for sufficiently large negative T-values (Smith et al., 2001). This result was later exploited to attempt to justify the behavior of some rock and glass material samples tested under mixed-mode loading conditions (Awaji and Sato, 1978; Khan and Al-Shayea, 2000; Chang et al., 2002; Aliha et al., 2006; Ayatollahi and Aliha, 2009a).

By means of a FFM approach based on the coupling of a tensile stress condition with an incremental energy requirement, in the present work it is shown that below a critical negative threshold for $T = T^{**} < 0$, the shear contribution to the ERR starts to prevail as mode II-loading conditions are approached. Theoretical predictions show a jump to infinitesimal quantities as concerns the critical kinking angle and the crack advance, and a unit limit value for the ratio between K_{IIf} and

K_{Ic}. As T further decreases, the shear energy dominated zone enlarges, giving rise to a smooth limit-behavior over the whole range of mode-mixities.

FFM predictions could be modified by assuming a fracture energy dependent on the mode-mixity, as commonly done in interface fracture mechanics (Hutchinson and Suo, 1992; Liechti and Chai, 1992; Banks-Sills and Ashkenazi, 2000; Mantič et al., 2006). In this case, K_{IIf} can theoretically exceed K_{Ic} **as observed in different experimental tests concerning polymeric materials (Smith et al., 2006), rocks (Awaji and Sato, 1978; Khan and Al-Shayea, 2000; Chang et al., 2002; Aliha et al., 2006), alumina and glass ceramics (Panasyuk et al., 1965; Shetty et al., 1986, 1987), and wood (Anaraki and Fakoor, 2010). Indeed, FFM results (and, more in general, results by any criterion involving a critical distance) reveal to be satisfactory only in case of a very brittle behavior, as long as the asymptotic expressions for the stress field and the SIFS related to a kinked crack are implemented.**

The analysis presented below is limited to a piecewise straight crack propagation, i.e. no curved crack-kinking (Amestoy and Leblond, 1992), in the framework of two-dimensional linear elasticity, i.e. no three-dimensional effects (Berto et al., 2011; Kotousov et al., 2013), where only the T-stress component parallel to the main crack plays a significant role, i.e. negligible constant (compressive) stresses perpendicular to the main crack (Isaksson and Ståhle, 2002; Li et al., 2009).

2. FFM criterion

The present FFM criterion (Carpinteri et al., 2009, 2010) is based on the assumption of a finite crack extension Δ and on the contemporaneous fulfilment of two conditions. The former is a stress requirement: the average circumferential

stress $\sigma_{\theta\theta}(r,\theta)$ on Δ, prior to the crack extension, must be greater than the material tensile strength σ_u. The latter is the energy balance: the integral of the strain ERR (or crack-driving force) G on Δ (i.e. the energy available for a crack increment Δ) must be higher than the fracture energy G_c times the crack increment. By referring to a cracked element with a polar reference system placed at the main crack tip (Fig. 1), FFM conditions write:

$$\begin{cases} \int_0^{\Delta} \sigma_{\theta\theta}(r,\theta)\mathrm{d}r \geq \sigma_u \Delta, \\ \int_0^{\Delta} \{[K_I^k(c,\theta)]^2 + [K_{II}^k(c,\theta)]^2\}\mathrm{d}c \geq K_{Ic}^2 \Delta. \end{cases} \tag{1}$$

Note that the energy balance in (1) is expressed in terms of the SIFs related to the kinked crack, K_I^k and K_{II}^k for mode I and mode II, respectively, by means of the well-known Irwin's relationships (assuming $K_I^k \geq 0$ and plain strain conditions):

$$G = G_I + G_{II} = \frac{(K_I^k)^2 + (K_{II}^k)^2}{E'}, \qquad G_c = \frac{K_{Ic}^2}{E'}, \tag{2}$$

where $E' = E/(1-\nu^2)$, E being Young's modulus and ν Poisson's ratio of the material.

Once θ is fixed, for monotonically decreasing $\sigma_{\theta\theta}(r,\theta)$ and monotonically increasing $G(c,\theta)$ functions (as supposed in the present analysis), the lowest load satisfying the inequalities in (1) is achieved when the equal sign holds.

2.1. Stress field and SIFs for kinked cracks

In order to implement FFM, the the expressions for the stress and the SIFs related to a kinked crack to be inserted into system (1) are invoked. By taking T-stress effects into account, the circumferential stress field $\sigma_{\theta\theta}(r,\theta)$ at the main crack tip can be approximated as (see Fig.1 with $c = 0$):

$$\sigma_{\theta\theta}(r,\theta) = \frac{K_I}{\sqrt{2\pi r}} f^I_{\theta\theta}(\theta) + \frac{K_{II}}{\sqrt{2\pi r}} f^{II}_{\theta\theta}(\theta) + T\sin^2\theta, \tag{3}$$

where K_I and K_{II} are the SIFs related to the main crack, whereas $f^I_{\theta\theta}$ and $f^{II}_{\theta\theta}$ are the corresponding angular functions, cf. Seweryn (1998).

On the other hand, by dimensional analysis concepts and the principle of superposition, the SIFs related to a kinked crack of length c can be expressed as (He et al., 1991; Amestoy and Leblond, 1992):

$$K^k_I(c,\theta) = \beta_{11}(\theta)K_I + \beta_{12}(\theta)K_{II} + \beta_1(\theta)T\sqrt{c}, \tag{4}$$

$$K^k_{II}(c,\theta) = \beta_{21}(\theta)K_I + \beta_{22}(\theta)K_{II} + \beta_2(\theta)T\sqrt{c}. \tag{5}$$

Approximating analytical expressions for the angular functions β are reported in Amestoy and Leblond (1992), and tabulated values can be found in Tada et al. (1985); Melin (1994); Fett et al. (2004). Note that β_2, β_{12} and β_{21} are odd functions, whereas β_1, β_{11} and β_{22} result to be even. For a null T-stress the last term in (4) and (5) vanishes, and the two expressions result thus independent of the crack length c.

Let us now introduce the fracture mode-mixity of the main crack $\psi = \arctan(K_{II}/K_I)$, the dimensionless kinked crack advance $\delta = \Delta/l_{ch}$ (with $l_{ch} = (K_{Ic}/\sigma_u)^2$) and the dimensionless T-stress, $\tau = T\sqrt{l_{ch}}/\sqrt{K_I^2 + K_{II}^2}$. In Fig. 2 the contributions of G_I and G_{II} evaluated by inserting (4) and (5) into (2) are presented for $\psi = 90^\circ$ (mode II loading conditions) and $\delta = 1/4\pi$. It can be observed that G_I decreases

as τ decreases, while the maximum of G_{II} keeps constant and it corresponds to $\theta = 0^\circ$ (collinear crack propagation).

2.2. FFM implementation

As already stated, at incipient failure ($K_I = K_{If}$), the coupled condition (1) becomes a system of two equations in two unknowns: the critical crack advancement δ_c and the failure load, implicitly embedded in the K_{If} function.

The substitution of (3), (4) and (5) into (1) provides after some simple algebraic manipulations, cf. Cornetti et al. (2014):

$$\begin{cases} \dfrac{K_{If}}{K_{Ic}} = \dfrac{\sqrt{\delta}}{\overline{f}^I_{\theta\theta} + \tan\psi \overline{f}^{II}_{\theta\theta} + \bar{\tau}\sqrt{\delta}\sin^2\theta}, \\ \delta = \dfrac{(\overline{f}^I_{\theta\theta} + \tan\psi \overline{f}^{II}_{\theta\theta} + \bar{\tau}\sqrt{\delta}\sin^2\theta)^2}{(\overline{\beta}_{11} + \overline{\beta}_{12}\tan\psi + \overline{\beta}_{22}\tan^2\psi) + \dfrac{4\bar{\tau}\sqrt{\delta}}{3}(\overline{\beta}_1 + \overline{\beta}_2\tan\psi) + \dfrac{\bar{\tau}^2\delta}{2}(\beta_1^2 + \beta_2^2)}, \end{cases} \tag{6}$$

where $\overline{f}^i_{\theta\theta} = \sqrt{2/\pi} f^i_{\theta\theta}$ ($i = I, II$), $\bar{\tau} = \tau\sqrt{(1+\tan^2\psi)}$ and the following combinations of the SIF angular functions are defined:

$$\overline{\beta}_1 = \beta_1\beta_{11} + \beta_2\beta_{21}, \qquad \overline{\beta}_2 = \beta_1\beta_{12} + \beta_2\beta_{22}, \tag{7}$$

$$\overline{\beta}_{11} = \beta_{11}^2 + \beta_{21}^2, \qquad \overline{\beta}_{22} = \beta_{12}^2 + \beta_{22}^2, \qquad \overline{\beta}_{12} = 2(\beta_{11}\beta_{12} + \beta_{21}\beta_{22}). \tag{8}$$

Observe that, for given loading and structural properties, ψ and τ are fixed. In order to implement FFM, the latter equation in (6) should be firstly solved: a different crack advance δ corresponds to a different kinking angle θ. Each couple (δ, θ) must be substituted into the former equation: the actual crack advance δ_c

and critical kinking angle θ_c are those which minimize the K_{If} function. The relationship $K_{IIf} = \tan\psi K_{If}$ then provides the corresponding value for K_{IIf}.

3. Discussion on FFM results

The results obtained by the above FFM procedure are depicted in Figs. 3, 4 and 5. As can be extracted from Figs. 3 and 4, FFM predicts higher failure loads and critical kinking angles for decreasing negative T-stresses over the range $-0.3 \leq \tau \leq 0$. The crack advance results to be a smooth monotonically decreasing function of ψ (Fig. 5).

On the other hand, when $\tau = \tau^{**} \simeq -0.325$, it is observed that K_{IIf} does not increase any more for $\psi = 90^\circ$ (mode II-loading conditions), and the corresponding values for θ_c and δ_c jump from -68.75° and 0.5233, respectively, to infinitesimal quantities. The limit $\theta_c = 0^\circ$ can never be reached from a theoretical point of view (taking the imposed tensile stress condition into account), since the angular function $f^{II}_{\theta\theta}$ would vanish, leading to a null circumferential stress. If one keeps on decreasing τ, results start to converge to the above mentioned values in proximity of mode II, till a smooth transition is observed over the full range of mode mixities ψ. Observe that the ratio K_{IIf}/K_{Ic} never exceeds the unit value (Fig. 3).

The following explanation to this behavior can be provided: the contribution of G_I in the energy balance of system (1) decreases as T decreases, but still remains dominant (as it happens for positive T-stress) over the range $-0.325 < \tau \leq 0$. Indeed, starting from $\tau^{**} \simeq -0.325$ and $\psi = 90^\circ$, the maximum energy available for a crack advance is provided by G_{II} for an infinitesimal angle (Fig. 2). In order for the stress requirement in (1) to match this condition, the crack advance must become infinitesimal too, so that tensile stresses result to be high enough.

The present behavior can not be detected by stress-based approaches, such as MTS criterion (Smith et al., 2001), **which is based on** the simple condition $\sigma_{\theta\theta}(r = r_c) \geq \sigma_c$, with $r_c = l_{ch}/2\pi$. In Smith et al. (2001) it was found that, even for large negative τ, the failure load keeps on increasing continuously and the kinking angle decreases uniformly in modulus. The explanation of this trend is quite straightforward: for a fixed critical distance, circumferential stresses decrease as T decreases, as it immediately follows from (3).

A comparison with $ad-hoc$ experimental results would reveal as fundamental to understand which is the real behavior observed from a testing procedure. **Indeed, almost all experiments on brittle polymeric materials involve either a positive or a moderate negative T-stress so that $\tau > -0.3$ (Erdogan and Sih, 1963; Williams and Ewing, 1972; Carpinteri et al., 1979; Ueda et al., 1983; Maccagno and Knott, 1989; Ayatollahi and Aliha, 2009b; Saghafi et al., 2013). Under these assumptions, FFM has already been proven to furnish accurate result (Cornetti et al., 2014). To the best of the authors' knowledge, the only significant data set refers to PMMA samples tested in Smith et al. (2006) under specific mode II loading conditions: in this case it was found that $K_{IIf}/K_{Ic} \simeq 1.21$ and $\theta_c \simeq -55.2°$, for $\tau \simeq -0.41$. It should be noted however that some scattering on experimental results was found during tests and that the curvature of the crack path was considerable, as observed by the authors themselves.**

Furthermore, disk specimens subjected to diametral compression often show a ratio $K_{IIf}/K_{Ic} > 1$ in the mode II-dominated zone (even for τ lower in modulus than -0.3) for some materials such as rocks (Awaji and Sato, 1978; Khan and Al-Shayea, 2000; Chang et al., 2002; Aliha et al., 2006), and alu-

mina and glass ceramics (Panasyuk et al., 1965; Shetty et al., 1986, 1987; Awaji and Kato, 1999). As already outlined in Cornetti et al. (2014), since rock materials are less brittle than polymeric materials (i.e. they present a higher l_{ch}), the related critical distance results larger and T-stress effects become more significant. On the other hand, if the critical length (described quantitatively by l_{ch}) is not sufficiently small with respect to the notch depth a, ($l_{ch}/a \simeq 1.7$ and 1.3, for instance, for the limestone and marble samples tested in Khan and Al-Shayea (2000) and Aliha et al. (2006), respectively), which in turn has to be sufficiently small with respect to the characteristic dimension of the specimen, the theory of critical distances can not be implemented accurately by simple asymptotic expansions (3), (4) and (5). Moreover, in these cases a complete analysis would require the inclusion of friction, of the influence of the root radius (McClintock (1963); Cotterell (1972)), and the implementation of a different mode of fracture (sliding and not opening), as suggested in Rao et al. (2003). Further studies are in progress. Similar arguments hold for polycrystalline ceramics: past studies showed that crack-surface resistances arising from grain interlocking and abrasion were the main sources of the increased fracture resistance in mode II, Singh and Shetty (1989); Rosenfield and Madjumar (1992).

The fact that K_{IIf}/K_{Ic} can exceed the unit value seems however to emerge clearly from some experiments. In order to justify this trend by FFM, let us observe that estimates of the toughening of elements under shear should consider possible local plastic and viscoelastic dissipation, crack face asperity shielding and frictional effects. In other words, the assumption of G_c to be constant is reasonable only if the G_I-contribution prevails in (2), whereas a larger amount of dis-

sipated energy should be associated to crack kinking dominated by G_{II}, typically occurring for $\theta \simeq 0^\circ$. This point has been largely investigated in the framework of interface fracture mechanics, where the interface fracture toughness was found to be even more than ten times greater as mode II is approached (Hutchinson and Suo, 1992; Liechti and Chai, 1992; Banks-Sills and Ashkenazi, 2000; Mantič et al., 2006). In order to overcome this drawback, one of the most implemented fracture criterion writes (Hutchinson and Suo, 1992):

$$\frac{G_I}{G_{Ic}} + \frac{G_{II}}{G_{IIc}} = 1, \tag{9}$$

where $G_{IIc} = G_{Ic}/\gamma$ has the interpretation of pure mode II toughness and γ is a parameter weighting the mode II-contribution. It vanishes for $\gamma \to 0$, whereas $\gamma = 1$ corresponds to an ideally brittle material. Note that the condition $\gamma \to 0$ provides the basis for the well-known $K_{II}^k = 0$ criterion proposed on the basis of simple symmetry arguments (Goldstein and Salganik, 1974; Amestoy and Leblond, 1992; Becker et al., 2001), and that an equivalent relationship to (9) was adopted in Seweryn (1998) **and suggested in Leguillon and Murer (2008)**.

In order to improve FFM predictions, from an equivalent point of view, one could consider the following modified ERR instead of G in (2):

$$\overline{G} = G_I + \gamma G_{II}. \tag{10}$$

By summarizing, Fig. 6 shows FFM results for pure mode I and mode II loading conditions, over the range $-1 \leq \tau \leq 1$. Predictions (represented by continuous lines) are obtained by setting $\gamma = 1$ in (10), i.e. by considering the classical ERR (2). On the other hand, if the limit case $\gamma = 0$ is implemented in (10), both the failure load and the critical kinking angle keep on increasing continuously for

decreasing T (dashed lines).

Results have been applied to PMMA samples tested in (Smith et al., 2006), showing an acceptable agreement as concerns the load (the mean percentage error being nearly -12%) and a significant deviation as regards the angle ($+13^\circ$). On the other hand, FFM predictions on data related to a positive T-stress, also reported in Fig. 6 for the sake of completeness, reveal to be satisfactory.

4. Conclusions

Effects of negative T-stress on brittle fracture of cracked elements were investigated by means of FFM. A competition between mode *I* and mode *II* contributions to the strain ERR was observed: for sufficiently large negative T-values, the latter prevails affecting the failure load and the critical kinking angle in the mode *II*-dominated zone. Predictions are in contrast with those provided by criteria based on simple stress considerations and showing monotonically increasing functions of the failure load and the kinking angle as T decreases. The idea of modifying FFM results by considering a mode-mixity dependent fracture toughness was furnished: this assumption takes the larger dissipated energy due to shear fracture mechanisms into account. **Due to the difficulties in performing tests under prevalent mode II loading conditions and a sufficiently negative T-stress, only few experimental results are present in the literature. Therefore, to carry out ad-hoc mode *II* tests on very brittle materials, starting from the procedure proposed in Smith et al. (2006), emerges as an important task to further corroborate the present analysis. Eventually, it appears that the relatively brittle response of rocks and the behavior of alumina and glass ceram-**

ics cannot be described accurately by means of simple asymptotic theories involving a critical distance. In other words, the large ratios $K_{IIf}/K_{Ic} > 1$ detected experimentally cannot be imputable only to the negative T-stress contribution. In order to improve FFM predictions, the following steps are suggested: i) higher order terms should be included in the series expansions for the stress field and the SIFs related to a kinked crack; ii) the effects of rubbing of these materials during the failure mechanism has to be properly taken into account.

Acknowledgements

Authors wish to thank Prof. Cornetti for useful discussions on the present topic. The financial support of V Plan Propio de Investigación de la Universidad de Sevilla (Modalidad I.6C), the Spanish Ministry of Economy and Competitiveness and European Regional Development Fund (Project MAT2012-37387), the Junta de Andaluca and the European Social Fund (Project TEP-04051) are also gratefully acknowledged. Eventually, Dr. Alberto Sapora acknowledges the hospitality of Universidad de Sevilla, where this work has been mostly accomplished.

References

Aliha, M. R. M., Ashtari, R., Ayatollahi, M. R., 2006. Mode I and mode II fracture toughness testing for a coarse grain marble. Applied Mechanics and Materials 56, 181–188.

Amestoy, M., Leblond, J. B., 1992. Crack paths in plane situations -II. detailed form of the expansion of the stress intensity factors. International Journal of Solids and Strucutres 29, 465–501.

Anaraki, A., Fakoor, M., 2010. General mixed mode I/II fracture criterion for wood considering t-stress effects. Materials and Design 31 (2010) 44614469 31, 4461–4469.

Awaji, H., Kato, T., 1999. Criterion for combined mode I-II brittle fracture. Materials Transactions 40, 972–979.

Awaji, H., Sato, S., 1978. Combined mode fracture toughness measurement by the disc test. J Engng Mater Technol 100, 175–182.

Ayatollahi, M., Aliha, M., 2009a. Mixed mode fracture in soda lime glass analyzed by using the generalized MTS criterion. International Journal of Solids and Structures 46, 311–321.

Ayatollahi, M. R., Aliha, M. R. M., 2009b. Analysis of a new specimen for mixed mode fracture tests on brittle materials. Engineering Fracture Mechanics 76, 1563–1573.

Banks-Sills, L., Ashkenazi, D., 2000. A note on fracture criteria for interface fracture. International Journal of Fracture 103, 177–188.

Becker, T. L., Cannon, R. M., Ritchie, R. O., 2001. Finite crack kinking and T-stresses in functionally graded materials. International Journal of Solids and Structures 38, 5545–5563.

Berto, F., Lazzarin, P., Kotousov, A., Harding, S., 2011. Out-of-plane singular stress fields in V-notched plates and welded lap joints induced by in-plane shear load conditions. Fatigue Fract. Eng. Mater. Struct 34, 291–304.

Carpinteri, A., Cornetti, P., Pugno, N., Sapora, A., 2010. On the most dangerous V-notch. International Journal of Solids and Structures 42, 887–893.

Carpinteri, A., Cornetti, P., Pugno, N., Sapora, A., Taylor, D., 2008. A finite fracture mechanics approach to structures with sharp V-notches. Engineering Fracture Mechanics 75, 1736–1752.

Carpinteri, A., Cornetti, P., Pugno, N., Sapora, A., Taylor, D., 2009. Generalized fracture toughness for specimens with re-entrant corners: Experiments vs. theoretical predictions. Structural Engineering and Mechanics 32, 609–620.

Carpinteri, A., Cornetti, P., Sapora, A., 2011. Brittle failures at rounded V-notches: a finite fracture mechanics approach. International Journal of Fracture 172, 1–8.

Carpinteri, A., DiTommaso, A., Viola, E., 1979. Collinear stress effect on the crack branching phenomenon. Matériaux et Construction 12, 439–446.

Chang, S., Lee, C., Jeon, S., 2002. Measurement of rock fracture toughness under modes i and ii and mixed-mode conditions by using disc- type specimen. Engng Geology 66, 79–97.

Cornetti, P., N.Pugno, Carpinteri, A., D.Taylor, 2006. Finite fracture mechanics: a coupled stress and energy failure criterion. Engineering Fracture Mechanics 73, 2021–2033.

Cornetti, P., Sapora, A., Carpinteri, A., 2014. T-stress effects on crack kinking in finite fracture mechanics. Engineering Fracture Mechanics 132, 169–176.

Cotterell, B., 1972. Brittle fracture in compression. International Journal of Fracture Mechanics 8, 195–208.

Cotterell, B., Rice, J. R., 1980. Slightly curved or kinked cracks. International Journal of Fracture 16, 155–169.

Erdogan, F., Sih, G. C., 1963. On the crack extension in plates under plane loading and transverse shear. Journal of Basic Engineering 85, 519–525.

Fett, T., Pham, V. B., Bahr, H. A., 2004. Weight functions for kinked semi-infinite cracks. Engineering Fracture Mechanics 71, 1987–1995.

Goldstein, R., Salganik, R., 1974. Brittle fracture of solids with arbitrary cracks. International Journal of Fracture 10, 507–523.

Gupta, M., Alderliesten, R., Benedictus, R., 2015. A review of T-stress and its effects in fracture mechanics. Engineering Fracture Mechanics 134, 218–241.

He, M. Y., Bartlett, A., Evans, A. G., Hutchinson, J. W., 1991. Kinking of a crack out of an interface: Role of in-plane stress. Journal of the American Ceramic Society 74, 767–771.

Hutchinson, J., Suo, Z., 1992. Mixed mode cracking in layered materials. Advances in Applied Mechanics 29, 63–191.

Isaksson, P., Ståhle, P., 2002. Mode II crack paths under compression in brittle solids a theory and experimental comparison. International Journal of Solids and Structures 39, 2281–2297.

Khan, K., Al-Shayea, N., 2000. Effect of specimen geometry and testing method on mixed iii fracture toughness of a limestone rock from Saudi Arabia. Rock Mech Rock Engng 33, 179–206.

Kosai, M., Kobayashi, A. S., Ramulu, M., 1993. Tear straps in airplane fuselage. In: Durability of Metal Aircraft Structures. Atlanta Technology Publications.

Kotousov, A., Lazzarin, P., Berto, F., Pook, L., 2013. Three-dimensional stress states at crack tip induced by shear and anti-plane loading. Engineering Fracture Mechanics 108, 65–74.

Leguillon, D., 1993. Asymptotic and numerical analysis of a crack branching in non-isotropic materials. European Journal of Mechanics A/Solids 12, 33–51.

Leguillon, D., 2002. Strength or toughness? A criterion for crack onset at a notch. European Journal of Mechanics A/Solids 21, 61–72.

Leguillon, D., Murer, S., 2008. Crack deflection in a biaxial stress state. International Journal of Fracture 150, 75–90.

Li, X., Liu, G., Lee, K., 2009. Effects of T-stresses on fracture initiation for a closed crack in compression with frictional crack faces. International Journal of Fracture 160, 19–30.

Liechti, K., Chai, Y., 1992. Asymmetric shielding in interfacial fracture under in-plane shear. Jounrnal of Applied Mechanics 59, 295–304.

Maccagno, T., Knott, J., 1989. The fracture behaviour of PMMA in mixed modes I and II. Engineering Fracture Mechanics 34, 65–86.

Mantič, V., Blázquez, A., Correa, E., París, F., 2006. Analysis of interface cracks with contact in composites by 2D BEM. In: Fracture and Damage of Composites, p. 189-248, Guagliano M, Aliabadi MH, editors. WIT Press.

McClintock, F. A., 1963. Discussion: on the crack extension in plates under plane loading and transverse shear (erdogan, f., and sih, g. c., 1963, asme j. basic eng., 85, pp. 519525). Journal of Basic Engineering 85, 525–527.

Melin, S., 1994. Accurate data for stress intensity factors at infinitesimal kinks. Journal of the Applied Mechanics 61, 467–470.

Panasyuk, V., Berezhnitskiy, L., Kovchik, S., 1965. Propagation of an arbitrarily oriented rectilinear crack during extension of a plate. Prikladnaya Mekhanika 1, 48–55.

Pugno, N., Ruoff, R., 2004. Quantized fracture mechanics. Philosophical Magazine 84, 2819–2845.

Rao, Q., Sun, Z., Stephansson, O., Li, C., Stillborg, B., 2003. Shear fracture (mode II) of brittle rock. International Journal of Rock Mechanics and Mining Sciences 40, 355–375.

Rosenfield, A., Madjumar, B., 1992. Fracture Toughness Evaluation of Ceramic Bonds using a Chevron-Notch Disk Specimen . In: Chevron-Notch Fracture Test Experience: Metals and Non Metals, K.R.Brown and I. Baratta, Eds . American Society for Testing and Materials.

Saghafi, H., Zucchelli, A., Minak, G., 2013. Evaluating fracture behavior of brittle polymeric materials using an IASCB specimen. Polymer Testing 32, 133–140.

Sapora, A., Cornetti, P., Carpinteri, A., 2013. A finite fracture mechanics approach to V-notched elements subjected to mixed-mode loading. Engineering Fracture Mechanics 97, 216–226.

Seweryn, A., 1998. A non-local stress and strain energy release rate mixed mode fracture initiation and propagation criteria. Engineering Fracture Mechanics 59, 737–760.

Shetty, D., Rosenfield, A., W.H.Duckworth, 1986. Mixed-mode fracture of ceramics in diametral compression. Journal of the American Ceramic Society 69, 437–443.

Shetty, D., Rosenfield, A., W.H.Duckworth, 1987. Mixed-mode fracture in biaxial stress state: Application of the diametral-compression (Brazilian disk) test. Engineering Fracture Mechanics 26, 825–840.

Singh, D., Shetty, D., 1989. Fracture toughness of polycrystalline ceramics in combined mode i and mode ii loading. Journal of the American Ceramic Society 72, 78–84.

Smith, D. J., Ayatollahi, M. R., Pavier, M. J., 2001. The role of T-stress in brittle fracture for linear elastic materials under mixed-mode loading. Fatigue Fract Engng Mater Struct 24, 137–150.

Smith, D. J., Ayatollahi, M. R., Pavier, M. J., 2006. On the consequences of T-stress in elastic brittle fracture. Proceedings of the Royal Society A 462, 2415–2437.

Tada, H., Paris, P. C., Irwin, G. R., 1985. The Stress Analysis of Cracks Handbook. Paris Productions Incorporated.

Ueda, Y., Ikeda, K., Yao, T., Aoki, M., 1983. Characteristics of brittle fracture under general combined modes including those under bi-axial tensile loads. Engineering Fracture Mechanics 18, 1131–1158.

Ševeček, O., Bermejo, R., Profant, T., Kotoul, M., 2014. Influence of the T-stress on the crack bifurcation phenomenon in ceramic laminates. Procedia Materials Science 3, 1062–1067.

Williams, J. G., Ewing, P. D., 1972. Fracture under complex stress - the angled crack problem. International Journal of Fracture Mechanics 8, 441–446.

List of Figures

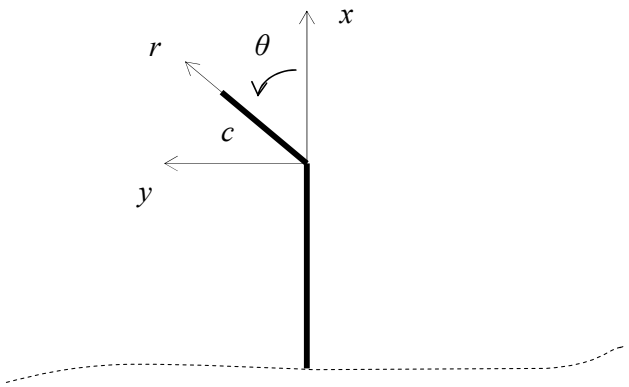

Figure 1: Cracked element with a kinked crack of length c.

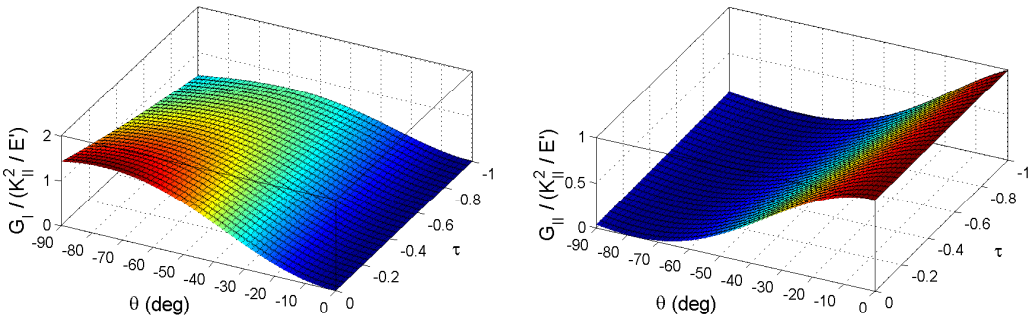

Figure 2: ERR contributions related to mode *I* and mode *II* as functions of θ and τ. Results refer to $\psi = 90°$ (mode *II* loading conditions) and $\delta = 1/4\pi$.

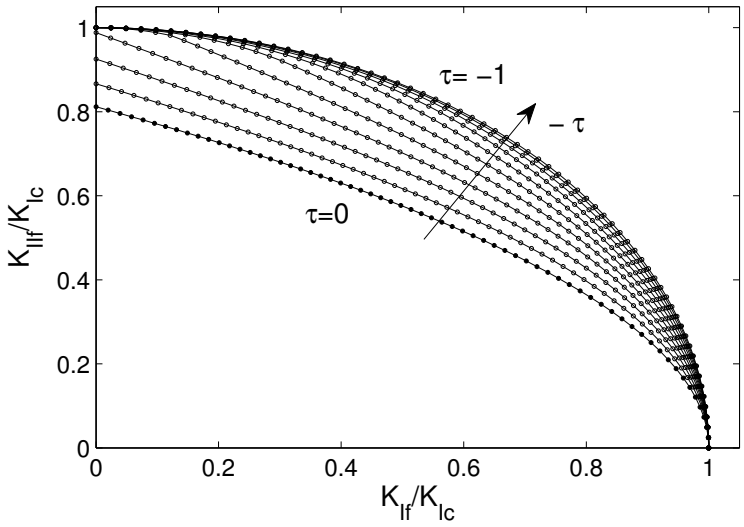

Figure 3: FFM fracture loci: effects of negative dimensionless T-stresses τ, ranging from 0 to -1 with a step equal to -0.1.

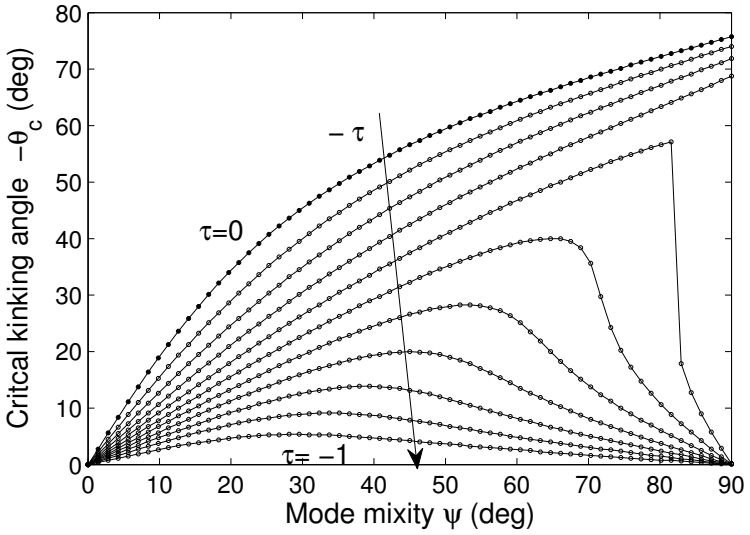

Figure 4: FFM critical kinking angle: effects of negative dimensionless T-stresses τ, ranging from 0 to -1 with a step equal to -0.1.

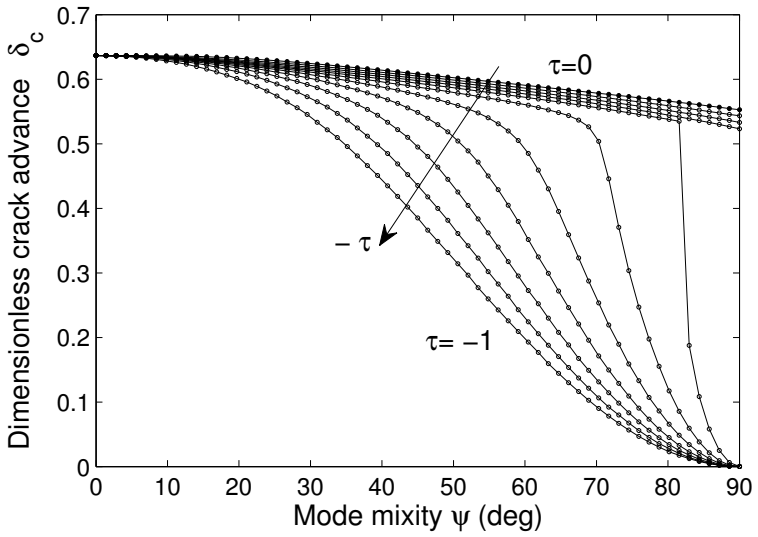

Figure 5: FFM critical crack advance: effects of negative dimensionless T-stresses τ, ranging from 0 to -1 with a step equal to -0.1.

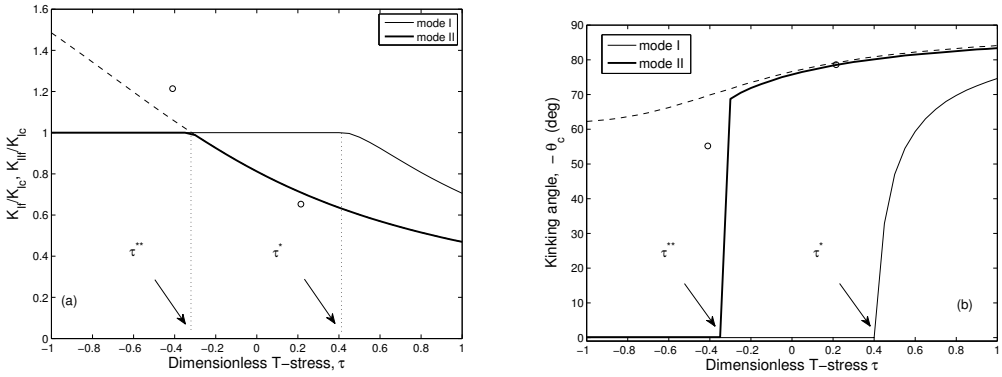

Figure 6: FFM predictions for pure mode *I* and mode *II* loading conditions: T-stress effects on (a) the critical SIFs and (b) the critical kinking angle. The dashed line refers to the predictions obtained by assuming $\gamma = 0$ in the modified ERR (10). The critical thresholds for mode I and mode II loading conditions are denoted by τ^{*} and τ^{**}. **Circles refer to the experimental data obtained by Smith et al. (2006)**